Dynamical Casimir effect in tunable superconducting circuits

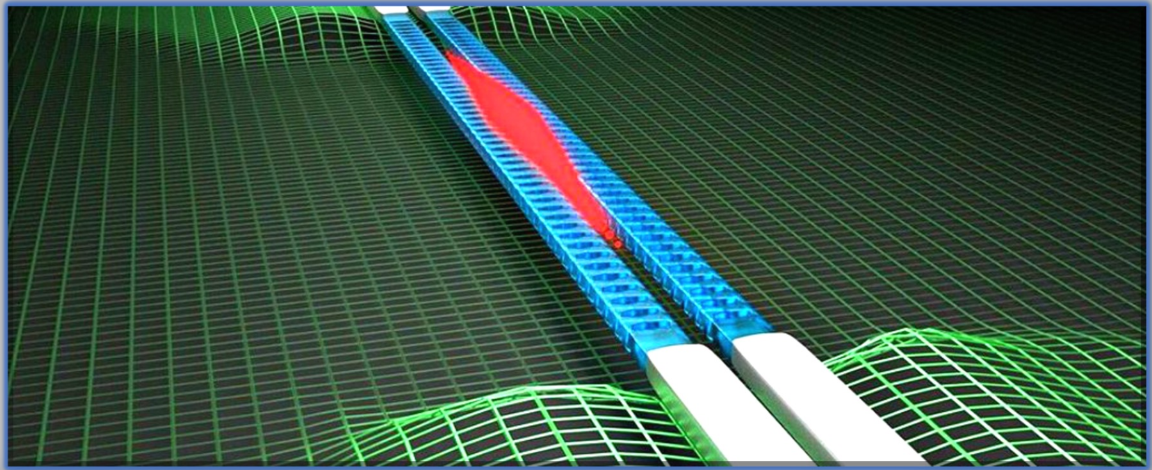

Paulo Maia Neto & Fernando Lombardo

Universidade Federal do Rio de Janeiro

UC SANTA BARBARA
Kavli Institute for
Theoretical Physics

Departamento de Física
.UBAexactas

Introduction

Vacuum excitation due to time dependent external conditions

Accelerated neutral objects

↓

DISSIPATIVE FORCES

PHOTON CREATION

DYNAMICAL CASIMIR EFFECT

Variation of electromagnetic properties of the media (conductivity, permittivity, etc)

Introduction

SOME INTUITION

classical

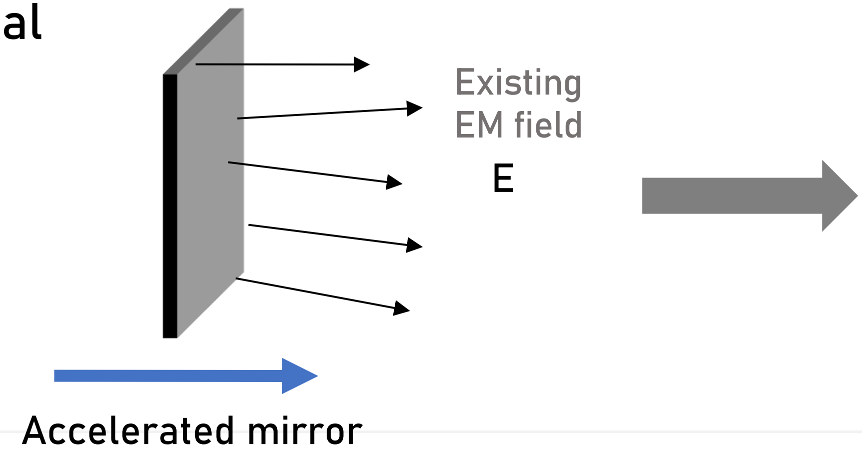

EM Wave

DYNAMICAL CASIMIR EFFECT

Introduction

SOME INTUITION

classical

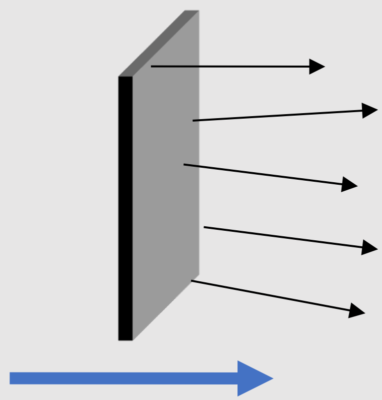

EM Wave

quantum

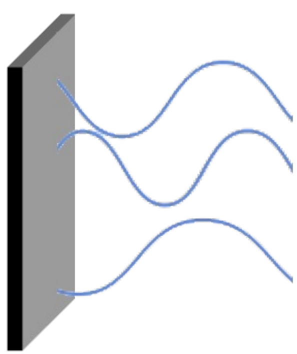

Photon creation

Reaction force on the mirror

Mirrors

OLD RESULTS FOR MOVING MIRRORS

Simplest case: massless scalar field in 1+1 D

Dirichlet boundary conditions

$$L = \frac{1}{2}\int_0^{L(t)} dx \left(\dot{\phi}^2 - \phi'^2\right) \longleftarrow \phi(t,0) = \phi(t,L(t)) = 0$$

$$\Big\downarrow$$

Static equidistant spectrum

Mirrors

OLD RESULTS FOR MOVING MIRRORS

Simplest case: massless scalar field in 1+1 D

$$L = \frac{1}{2}\int_0^{L(t)} dx \left(\dot{\phi}^2 - \phi'^2\right)$$

Dirichlet boundary conditions

$$\phi(t,0) = \phi(t,L(t)) = 0$$

$$\phi(t,x) = \sum_n q_n(t) \sin\left(\frac{n\pi x}{L(t)}\right)$$

Static equidistant spectrum

Instantaneous basis (useful for intermediate calculations, no intention to define N(t)!)

Set of coupled harmonic oscillators

SECULAR EFFECTS

external frequency = eigenfrequency

DYNAMICAL CASIMIR EFFECT

Equidistant spectrum

All modes are coupled

The number of particles created grows quadratically with t.

Total energy in the cavity grows exponentially (Dodonov & Klimov 1996)

More general boundary conditions

Massive case → Non-equidistant spectrum

↓

Cavities in 3+1 dimensions

Possibility of parametric resonance for a single mode (or a few modes)

↓

Exponential growth

Crocce, Dalvit & Mazzitelli, 1999, 2000. Numerics: P. Villar & A. Soba, PRE 2017

Very difficult to observe…

Rate of photon production by a single oscillating mirror *in vacuum*

$$\frac{N}{T} = \frac{A}{60\pi^2}\frac{\Omega^3}{c^2}\left(\frac{v_{max}}{c}\right)^2$$

V = Ω . a

$$\frac{v_{max}}{c} = 10^{-7} \quad \Omega = 10GHz \quad A = 10cm^2$$

1 photon/day!!

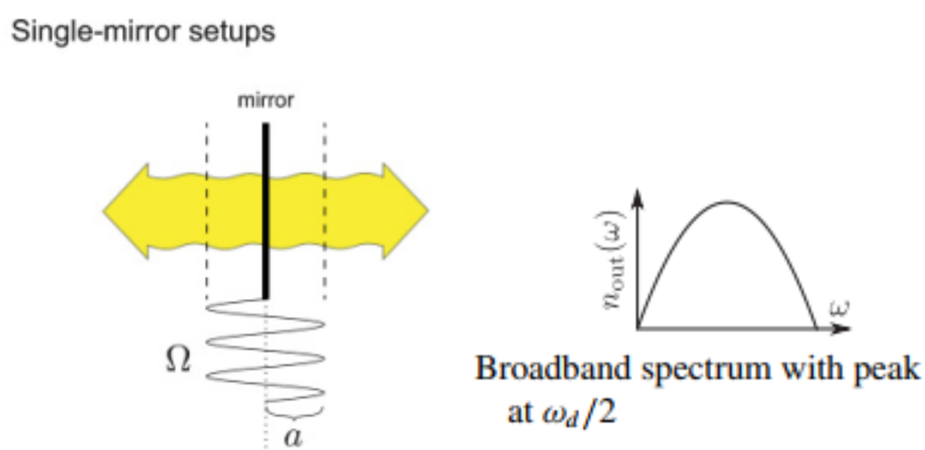

[1] G.T. Moore, J. Math. Phys. 11, 2679 (1970)

[2] A. Lambrecht, M.T. Jaekel and S. Reynaud, Phys. Rev. Lett.77, 615 (1996)

For *cavities* the situation is better due to parametric resonace… but still difficult

$$N = e^{\eta\epsilon\Omega t}, \eta = O(1)$$

$$N_{max} \simeq e^{\epsilon Q} \leq e^{10^{-8} Q}$$

- In order to produce 5 GHz photons, we need mechanical oscillations with 10GHz
- Actual limit: 6GHz

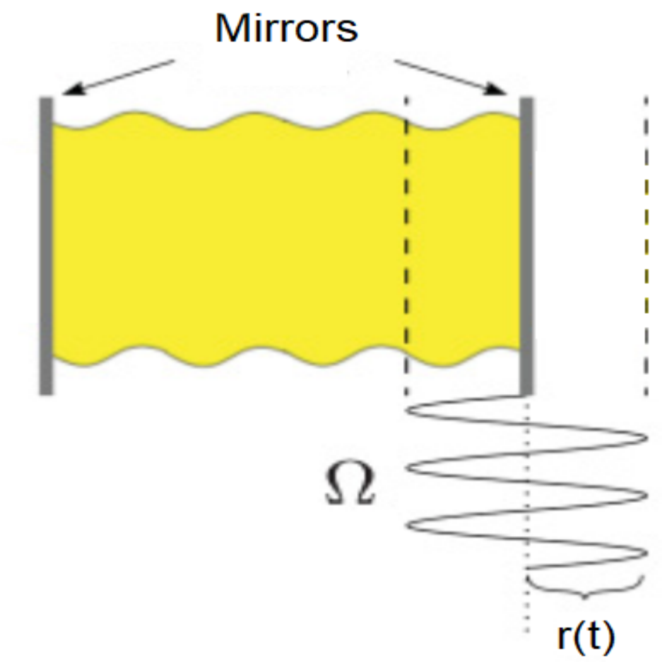

One EM mode

If $r(t) = a\, L\, \mathrm{Sin}(\Omega\, t)$, $a << 1$, $\Omega = 2\, \boldsymbol{\omega}_k$

Parametric resonance

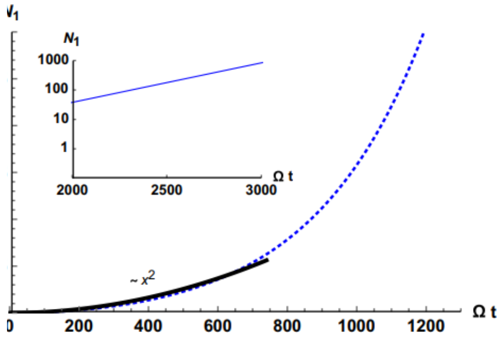

$\langle 0|\, N_k |0\rangle = \mathrm{Sinh}^2(a\boldsymbol{\omega}_k\, t/2)$ Photon generation

More modes: infinite harmonic oscillators

Resonance conditions:

- $\Omega = 2\, \boldsymbol{\omega}_k$ photon pair creation in mode k
- $\Omega = \boldsymbol{\omega}_k + \boldsymbol{\omega}_j$ pair creation in modes k and j
- $\Omega = |\boldsymbol{\omega}_k - \boldsymbol{\omega}_j|$ scattering between modes j and k

P I Villar, A. Soba, Phys. Rev. E 96, 013307 (2017)

2 moving mirrors

“interference” effects in the particle creation rate

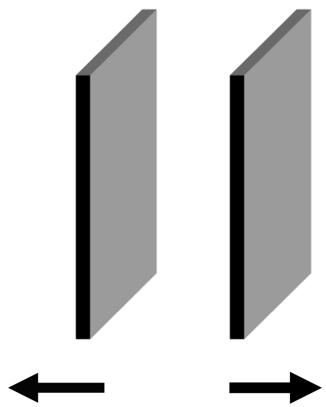

“breathing” mode

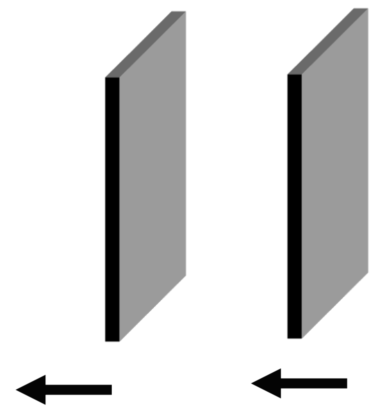

“shaker” mode

Mainly studied for Dirichlet fields in 1+1

Dalvit & Mazzitelli (1999) – Villar, Soba & Lombardo (fully numerical approach (2017)

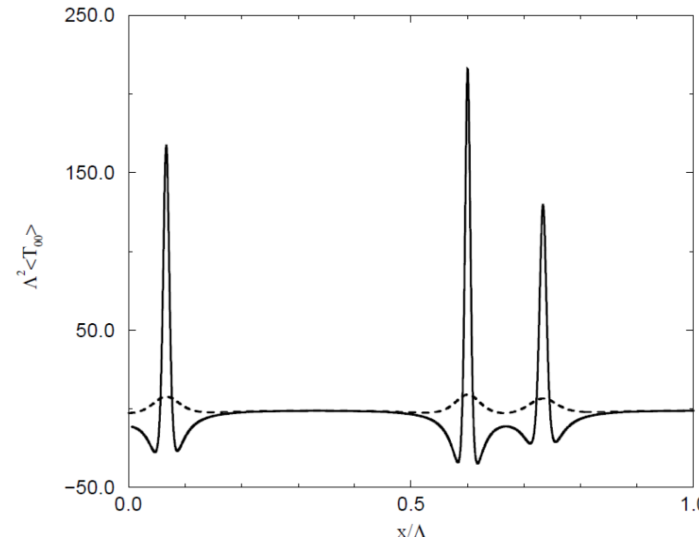

Secular behaviour for integer values of *q*

$$L(t) = \epsilon A_L \sin\left(\frac{q\pi t}{\Lambda}\right) \equiv 0 + \epsilon \delta L(t)$$

$$R(t) = \Lambda - \epsilon A_R \sin(\phi) + \epsilon A_R \sin\left(\frac{q\pi t}{\Lambda} + \phi\right) \equiv \Lambda + \epsilon \delta R(t)$$

shaker mode, q=3 (compared with 1 mirror oscilation)

Perturbation theory doesn't work

when *a* or *b* do not vanish

$$a \equiv \frac{\epsilon}{\Lambda}\frac{\pi}{2}\left[\frac{A_L}{\Lambda} + \frac{A_R}{\Lambda}(-1)^{q+1}\cos(\phi)\right]$$
$$b \equiv \frac{\epsilon}{\Lambda}\frac{\pi}{2}\frac{A_R}{\Lambda}(-1)^{q+1}\sin(\phi).$$

Method: conformal transformation → Moore equation → RG improved solution

Dalvit & Mazzitelli (1999) – Villar, Soba & Lombardo (2017)

The rate of particle creation depends strongly on the relation among the amplitudes, the frequency, and the phase difference in the mirrors' oscillations.

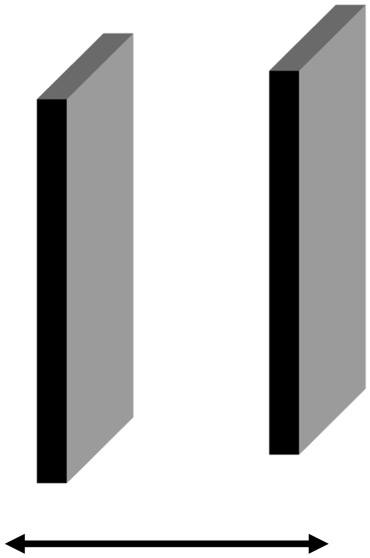

In some cases constructive interference **leads to exponential growth of particles** inside the cavity, while for other relations there exists destructive interference **with no vacuum radiation.**

Dalvit & Mazzitelli PARA (1999) – Villar, Soba & Lombardo PRA (2017)

EXPERIMENTAL VERIFICATION OF DCE (2011)

By applying a time-dependent magnetic flux through the SQUID we get a time-dependent inductance, which in turn produces a time-dependent boundary condition for the field in the waveguide

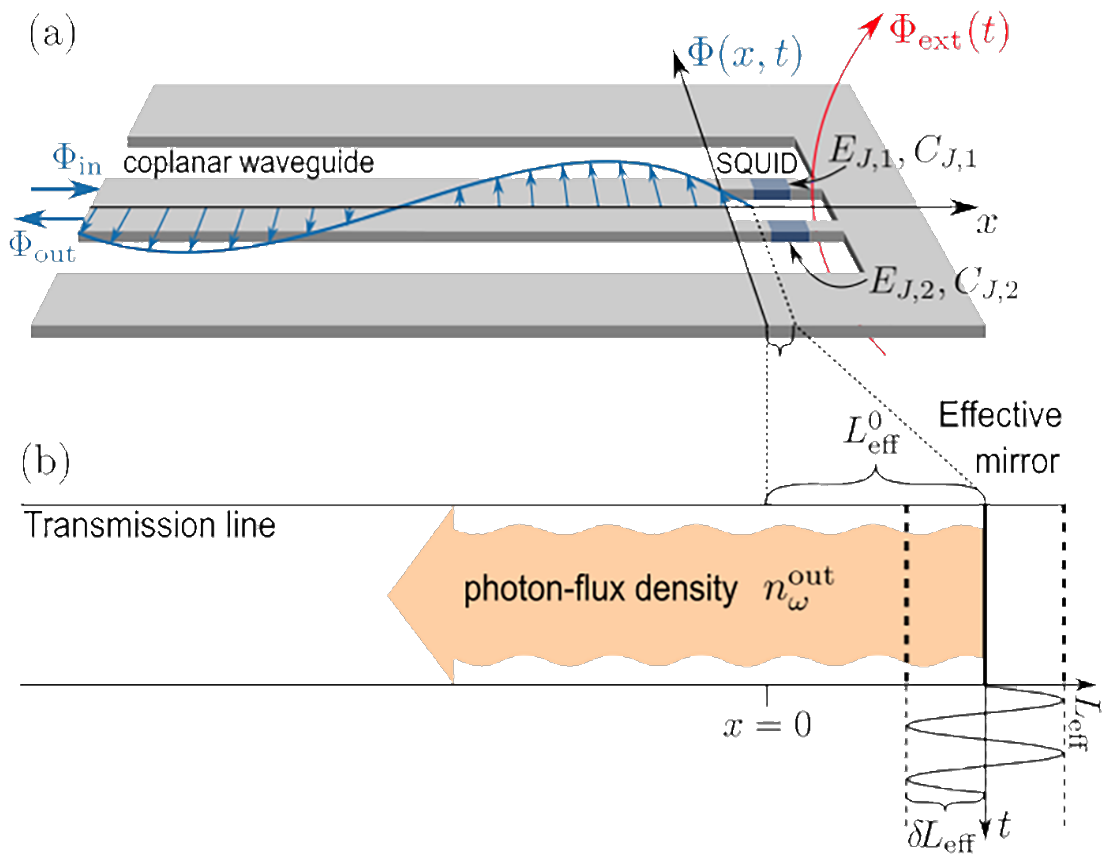

Modulated inductance of SQUID at high frequencies (> 10 GHz)

---

[4] J. R. Johansson, G. Johansson, C. M. Wilson, and F. Nori, Phys. Rev. Lett. 103, 147003 (2009)

[5] G. Johansson, A. Pourkabirian, M. Simoen, J. R. Johansson, T. Duty, F. Nori, and P. Delsing, Nature 479, 376 (2011)

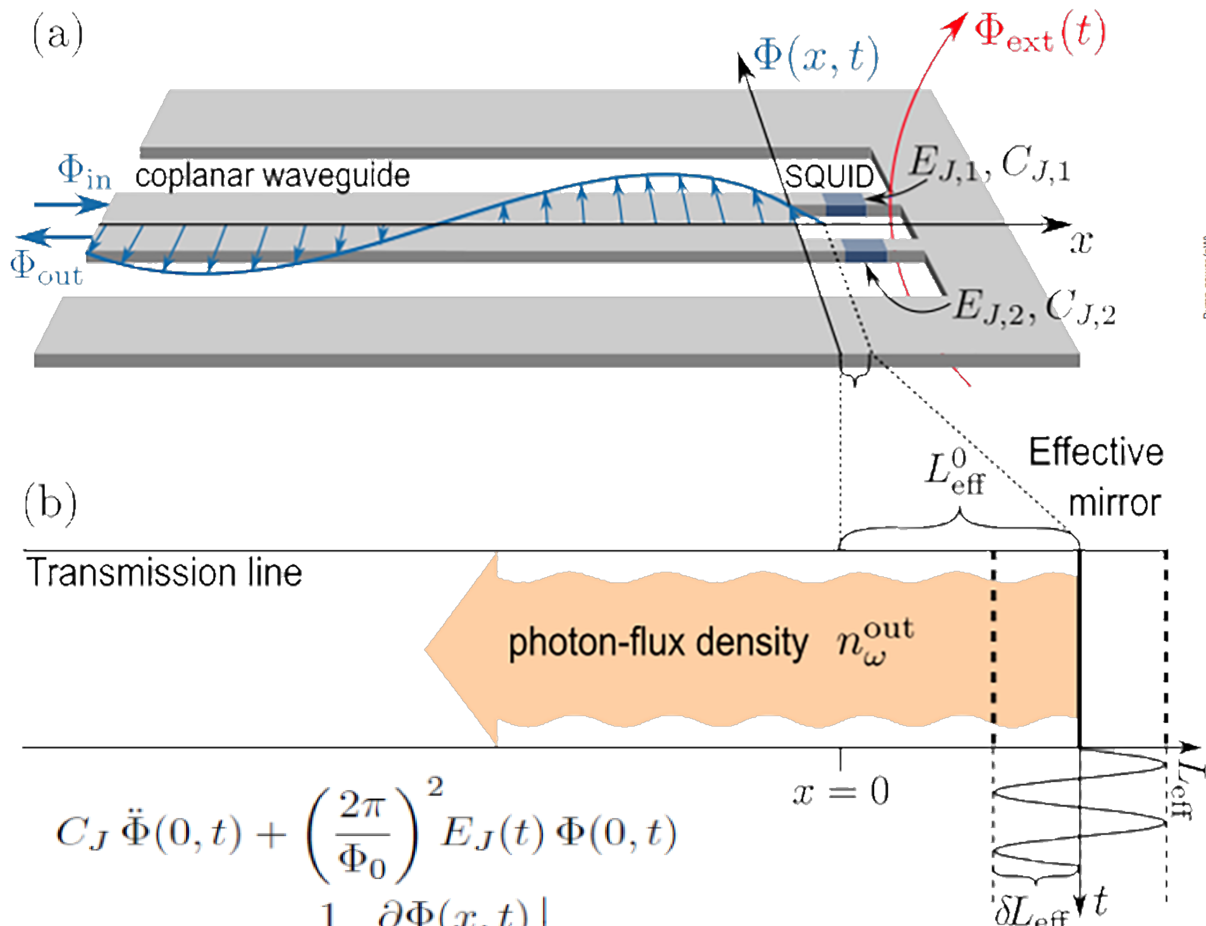

$$C_J\,\ddot{\Phi}(0,t) + \left(\frac{2\pi}{\Phi_0}\right)^2 E_J(t)\,\Phi(0,t) + \frac{1}{L_0}\,\frac{\partial \Phi(x,t)}{\partial x}\bigg|_{x=0} = 0$$

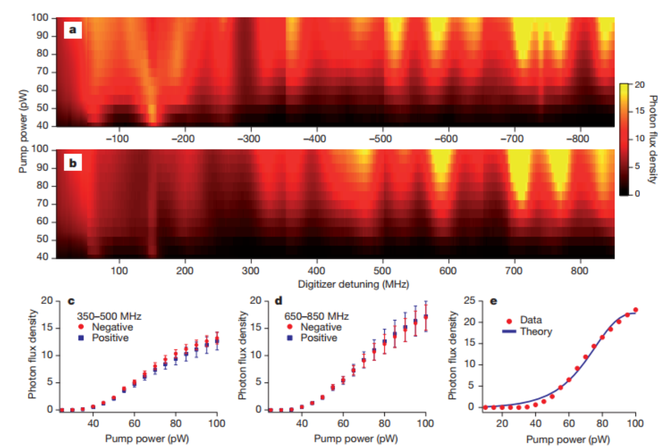

Time dependent boundary condition

DIFFERENT EXPERIMENTAL REALIZATIONS OF DCE

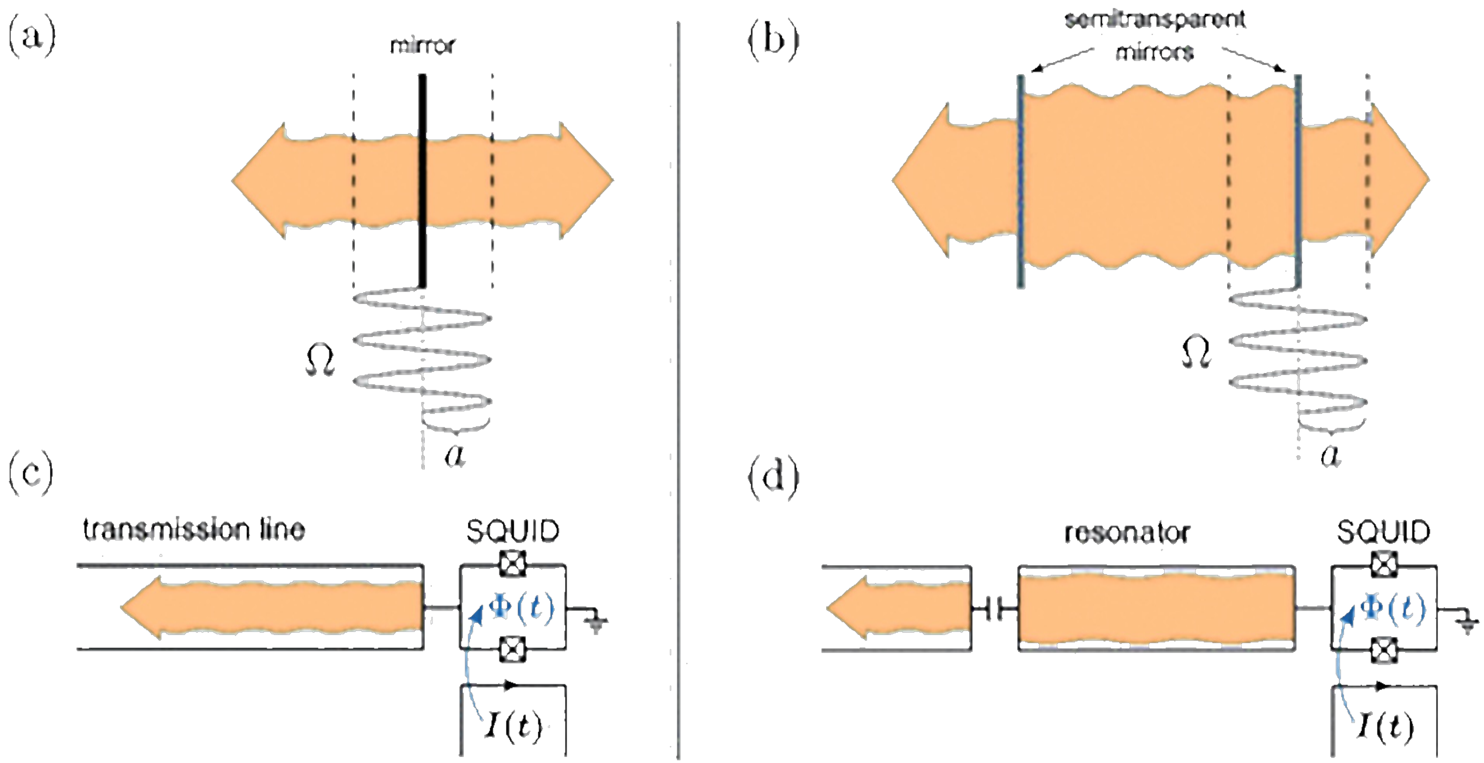

J. R. Johansson, G. Johansson, C. M. Wilson, and F. Nori, Phys. Rev. A 82, 052509 (2010).

MORE RECENT EXPERIMENTAL RESULTS
(doubly tunable resonator)

Particle creation with simultaneous excitation of both SQUIDs

Observation of interference effects.

$$\Omega_L = \Omega_R = 2k_n$$

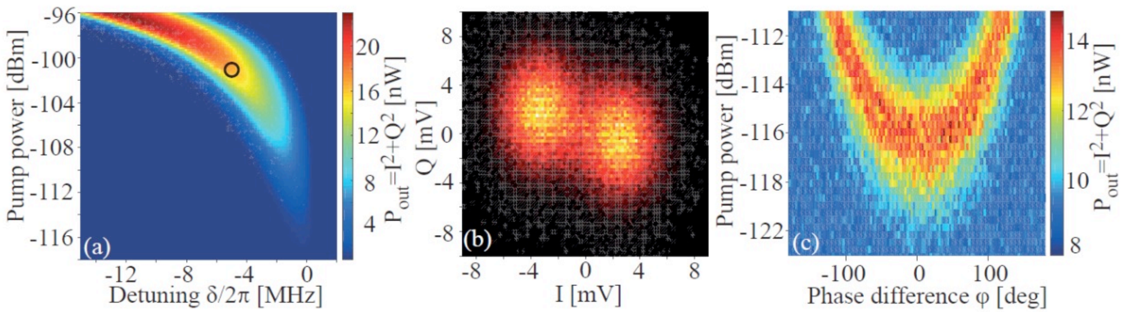

Figure 3. (a) Photon down-conversion. Measured with a single pump applied to the left flux line at the bias point $(0.3, 0.3)\,\Phi_0$. (b) Histogram taken at the point marked with a black circle in (a). We measure two π-shifted states. (c) Double-pump measurement, where the phase difference, φ between the pump signals is varied. Here the SQUID bias is $(0.2, 0.2)\,\Phi_0$ and the generated radiation for $\delta = -1\,\text{MHz}$ is displayed.

Svensson et al 2018

TUNABLE SUPERCONDUCTING CAVITY

Model

$$L_{\mathrm{cav}} = \left(\frac{\hbar}{2e}\right)^2 \frac{C_0}{2} \int_0^d dx(\dot{\phi}^2 - v^2 \phi'^2)$$

$$+ \left[\left(\frac{\hbar}{2e}\right)^2 \frac{2C_J}{2} \dot{\phi}_d^2 - E_J \cos f(t) \phi_d^2 \right],$$

Superconducting phase field: scalar field in the cavity

Cavity with capacitance C_0 and inductance L_0

$$v = 1/\sqrt{L_0 C_0}$$

Field propagation velocity

E_J and C_J Energy and capacitance of the SQUID en x = d

$$f(t) = f_0 + \theta(t)\theta(t_F - t)\epsilon \sin \Omega t,$$

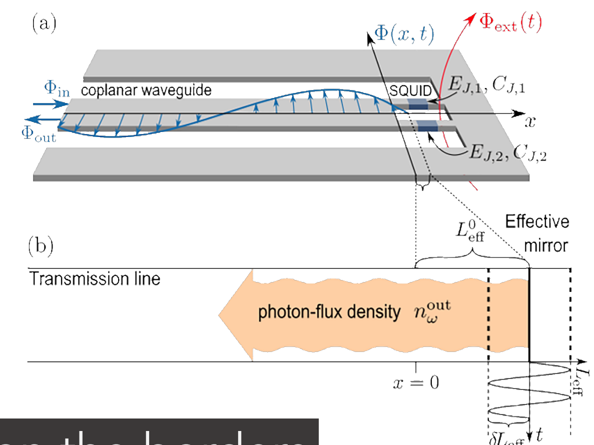

Quantum field in 1+1 dimensions with terms localized on the borders

Wustmann Shumeiko 2013

Model

$$\ddot{\phi} - v^2\phi'' = 0$$

$$\frac{\hbar^2}{E_C}\ddot{\phi}_d + 2E_J\cos f(t)\phi_d + E_{L,\mathrm{cav}}d\phi_d' = 0,$$

$$E_C = (2e)^2/(2C_J)$$

$$E_{L,\mathrm{cav}} = (\hbar/2e)^2(1/L_0 d)$$

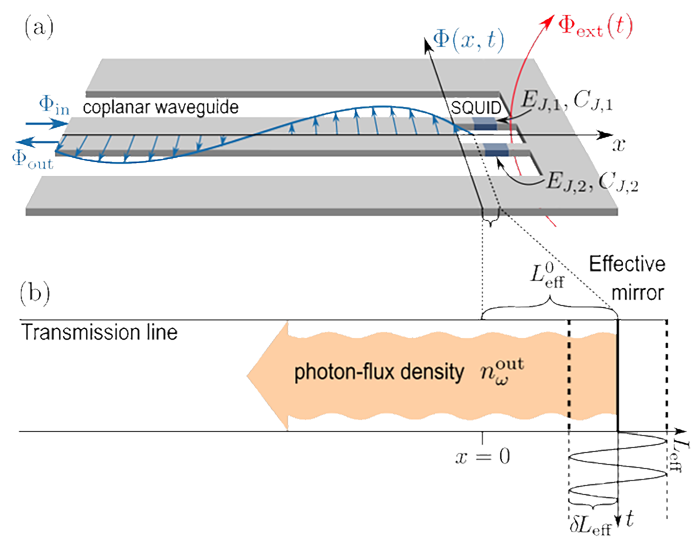

Unusual boundary conditions ⟷ localized degrees of freedom

PARTICLE CREATION IN A TUNABLE CAVITY

$$\phi(x,t) = \frac{2e}{\hbar}\sqrt{\frac{2}{C_0 d}}\sum_n q_n(t)\cos k_n x,$$

Expansion of the field in terms of modes of the static cavity

$$(k_n d)\tan k_n d = \frac{2E_J \cos f_0}{E_{L,\mathrm{cav}}} - \frac{2C_J}{C_0 d}(k_n d)^2$$

Equations that define the static spectrum

$$\ddot{q}_n + v^2 k_n^2 q_n = \frac{4E_J}{E_{L,\mathrm{cav}} M_n}\frac{v^2}{d^2}\epsilon\,\theta(t)\theta(t_F - t)\sin(f_0) \times \sin\Omega t\cos k_n d\sum_m q_m(t)\cos k_m d,$$

Field equations

Lombardo, Mazzitelli, Soba & Villar 2016, 2018

QUANTIZATION

$$\hat{q}_n(t) = u_n(t)\hat{a}_n + u_n^*(t)\hat{a}_n^\dagger,$$

$$u_n^{in}(t) = \frac{1}{\sqrt{2vk_n}} e^{-ivk_n t} \quad \text{for} \quad t < 0.$$

$$u_n^{in}(t) = \alpha_n u_n^{out}(t) + \beta_n u_n^{out\,*}(t),$$

$$\boxed{N_n = \langle 0_{in} | a_n^{out\,\dagger} a_n^{out} | 0_{in} \rangle = |\beta_n|^2.}$$

Particle number in mode n

SPECTRUM

$$k_n d \tan(k_n d) + \chi_0 (k_n d)^2 = V_0 \cos f_0.$$

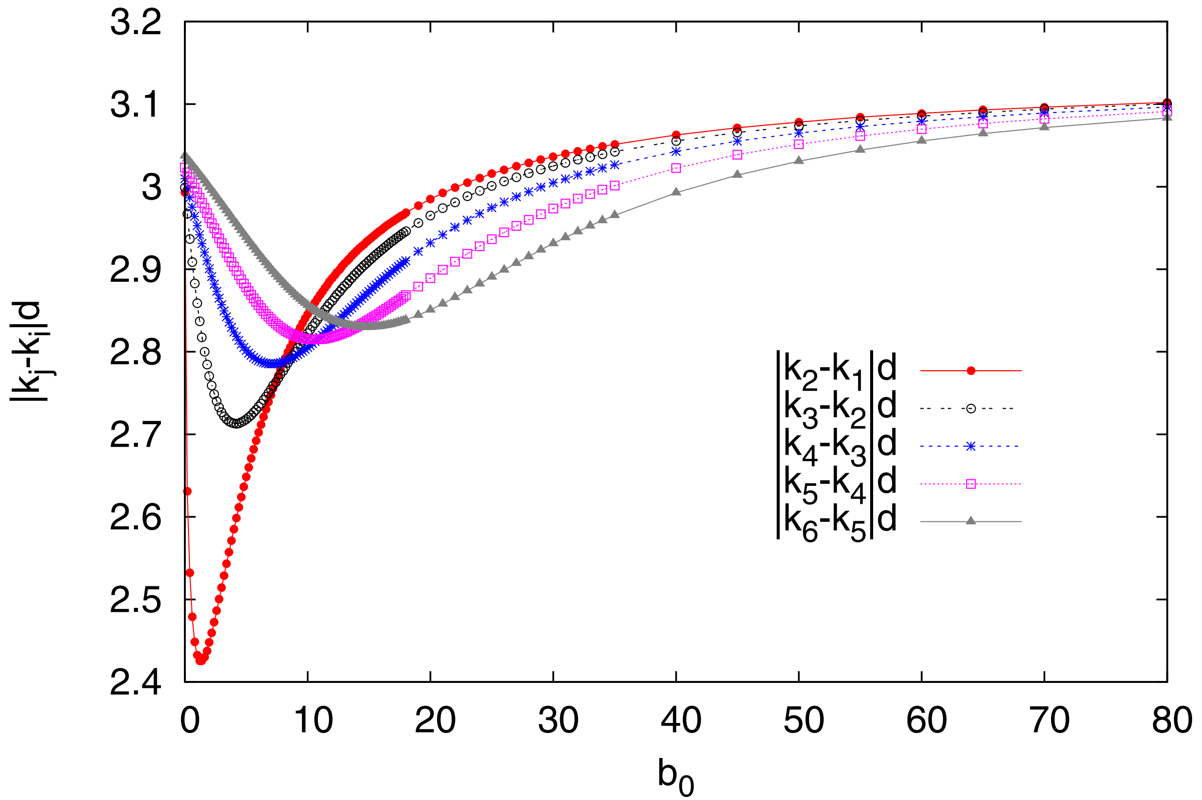

$b_0 = V_0 \cos f_0$

SPECTRUM: SUMMARY

- The spectrum is determined by the static parameters of the SQUID
- Parameters can be adjusted to have equidistant or non-equidistant spectra
- The space of parameters is richer and easier to adjust compared with the case of mirrors (would involve a manipulation of their electromagnetic properties)

ANALYTICAL RESULTS: Multiple Scale Analysis

$$\ddot{q}_n + \omega_n^2(t) q_n = \sum_{m \neq n} S_{nm}(t) q_m,$$

$$\omega_n(t) = k_n \left(1 - \alpha \frac{k_1^2}{k_n^2} \frac{\cos^2 k_n d}{M_n} \sin \Omega t \right)$$

$$S_{mn}(t) = \alpha k_1^2 \frac{\cos k_n d \cos k_m d}{\sqrt{M_n M_m}} \sin \Omega t$$

$$\alpha = \frac{4 E_J}{E_{L,\mathrm{cav}} k_1^2 d^2} \epsilon \ \sin(f_0).$$

$$q_n(t, \tau) = A_n(\tau) \frac{e^{-i k_n t}}{\sqrt{2 k_n}} + B_n(\tau) \frac{e^{i k_n t}}{\sqrt{2 k_n}}.$$

ANALYTICAL RESULTS: Multiple Scale Analysis

$$
\begin{aligned}
\frac{dA_n}{d\tau} = & -\frac{k_1^2}{k_n}\frac{\cos^2 k_n d}{2M_n} B_n \delta(\Omega - 2k_n) \\
& + \frac{k_1^2}{4}\sum_{m\neq n}\frac{\cos k_n d \cos k_m d}{\sqrt{k_n k_m M_n M_m}} \\
& \times \{A_m[\delta(k_n - k_m + \Omega) - \delta(k_n - k_m - \Omega)] \\
& - B_m \delta(k_n + k_m - \Omega)\},
\end{aligned}
$$

$$
\begin{aligned}
\frac{dB_n}{d\tau} = & -\frac{k_1^2}{k_n}\frac{\cos^2 k_n d}{2M_n} A_n \delta(\Omega - 2k_n) \\
& - \frac{k_1^2}{4}\sum_{m\neq n}\frac{\cos k_n d \cos k_m d}{\sqrt{k_n k_m M_n M_m}} \\
& \times \{B_m[\delta(k_m - k_n + \Omega) - \delta(k_m - k_n - \Omega)] \\
& + A_m \delta(k_n + k_m - \Omega)\}.
\end{aligned}
$$

Resonance conditions

$\Omega_{L,R} = 2k_n \quad \Omega_{L,R} = |k_n \pm k_j|$

NUMERICAL ANALYSIS

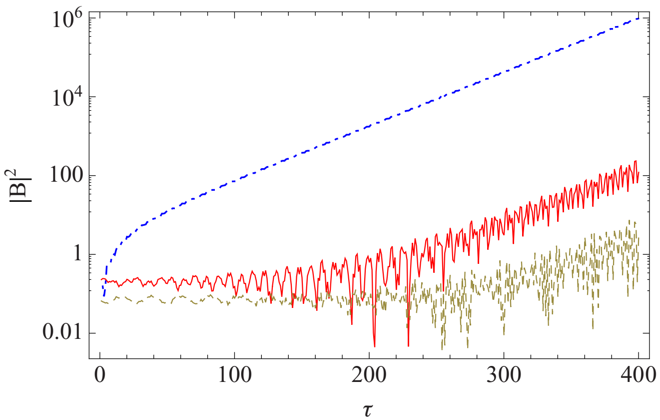

FIG. 3. Log plot for $|B_n|^2$ as a function of dimensionless time τ (time measured in units of d) for each mode of the field for a short temporal scale. Herein, we consider ten modes and excite the system by $\Omega = 2k_1$. The three first eigenfrequencies are $k_1 = 0.849$ (blue dot-dashed line), $k_2 = 3.281\,9$ (red solid line), and $k_3 = 6.140\,3$ (green dashed line).

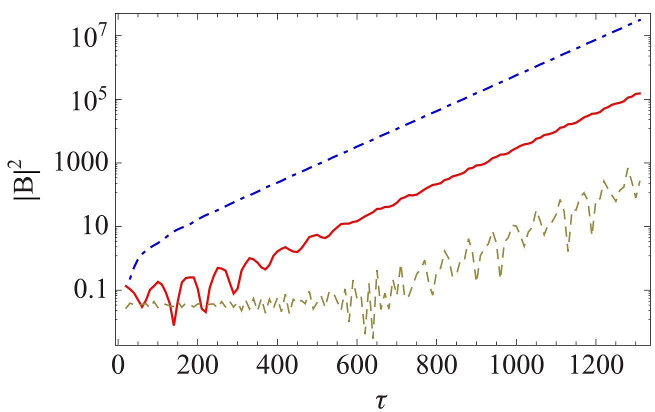

FIG. 8. Log plot for $|B_n|^2$ as a function of time for each mode of the field. Herein, we consider ten modes and excite the system by $\Omega = 2k_1$. The blue dot-dashed line corresponds to the field mode 1: $|B_1|^2$, the red solid line to field mode 2: $|B_2|^2$, and the green dashed one to $|B_3|^2$ for the field mode 3.

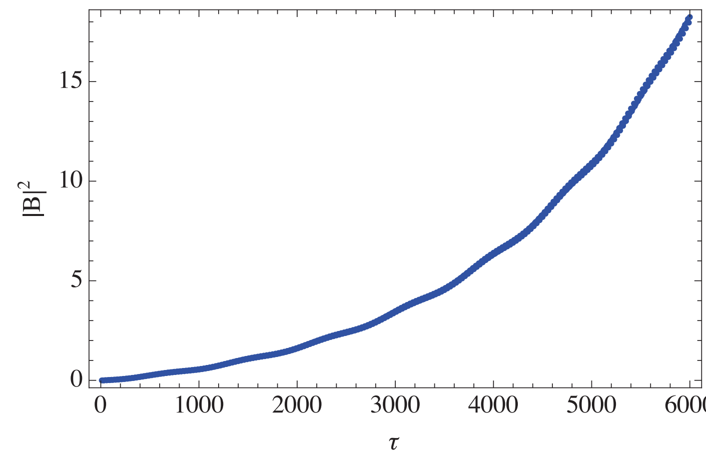

FIG. 9. Evolution of field mode 1 ($|B_1|^2$) for short dimensionless time scale under external driving $\Omega = 2k_1$. We can fit this behavior with a quadratic function.

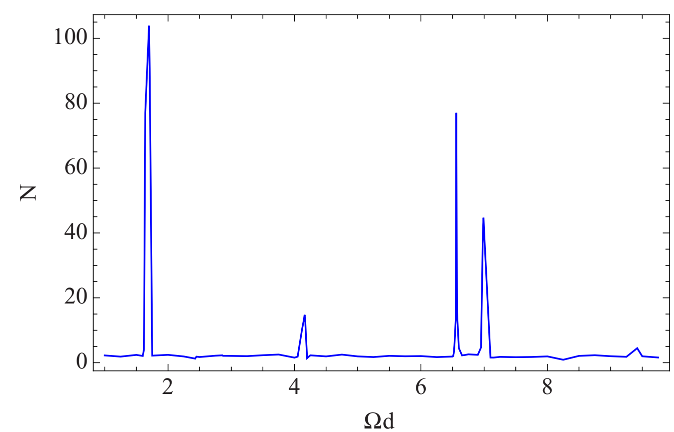

FIG. 7. Number of particles created as a function of the external dimensionless frequency Ωd. The eigenfrequencies (in units of $1/d$) are $k_1 d = 0.849\,5$, $k_2 d = 3.281\,9$, $k_3 d = 6.140\,3$, and $k_4 d = 9.093\,0$. We can see that the higher peak corresponds to $\Omega = 2k_1$ and the following to $\Omega = 2k_2$. Less important are $\Omega = k_1 + k_2$ and $\Omega = k_1 + k_3$.

CONCLUSIONS: DCE

- Numerical and analytical results for particle creation in a single or doubly tunable superconducting cavity (even an array)
- The description of the system involves generalized boundary conditions or degrees of freedom concentrated on the boundaries
- Parameters can be tunned to change the characteristics of the spectrum
- Rate of particle creation strongly depends on the eigenvalues and phases of the static eigenfunctions
- Interference effects by dephasing the external magnetic fields on both SQUIDs
- Analytical results based on Multiple Scale Analysis
- Numerical results confirm and extend analytical analysis

QUANTUM THERMODYNAMICS AND DCE

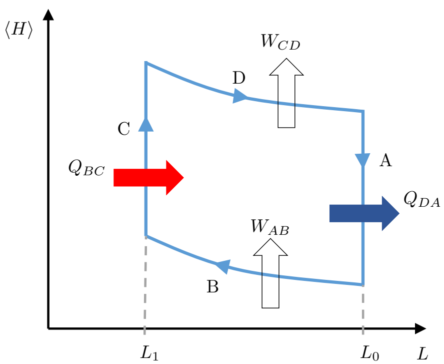

$$L(t) = L_0[1 - \epsilon\delta(t)]$$

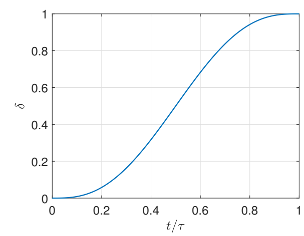

$$\delta(t) = 10(t/\tau)^3 - 15(t/\tau)^4 + 6(t/\tau)^5$$

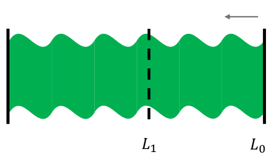

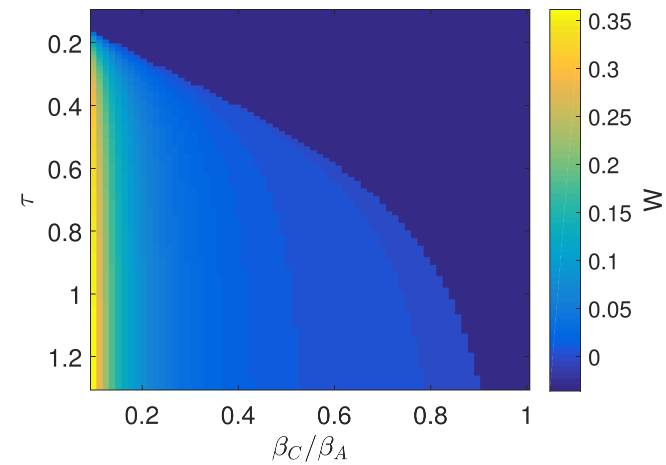

FIG. 7. Work extracted from the engine. We can identify regions where no work can be extracted from the Otto cycle. The compression ratio used is $\epsilon = 0.01$.

We analyze the efficiency of the quantum Otto cycle applied to a superconducting cavity. We consider its description in terms of a full quantum scalar field in a one-dimensional cavity with a time-dependent boundary condition that can be externally controlled to perform and extract work unitarily from the system. We study the performance of this machine when acting as a heat engine as well as a refrigerator. It is shown that, in a nonadiabatic regime, the efficiency of the quantum cycle is affected by the dynamical Casimir effect that induces a sort of quantum friction that diminishes the efficiency. We also find regions of parameters where the effect is so strong that the machine can no longer function as an engine since the work that would be produced is completely consumed by the quantum friction. However, this effect can be avoided for some particular temporal evolutions of the boundary conditions that do not change the occupation number of the modes in the cavity, leading to a highly improved efficiency.

Del Grosso, Lombardo, Mazzitelli & Villar, PRA 2022

Shortcut to adiabaticity in a cavity with a moving mirror

Shortcuts to adiabaticity constitute a powerful alternative that speed up time evolution while mimicking adiabatic dynamics. We described ***how to implement shortcuts to adiabaticity for the case of the superconducting phase field inside a cavity with a moving wall***, in 1 + 1 dimensions.

The approach is based on solution to the problem that exploits the conformal symmetry, and ***the shortcuts take place whenever there is no dynamical Casimir effect. We obtain a fundamental limit for the efficiency of an Otto cycle with the quantum field as a working system, that depends on the maximum velocity that the mirror can attain***. We describe possible experimental realizations of the shortcuts using superconducting circuits.

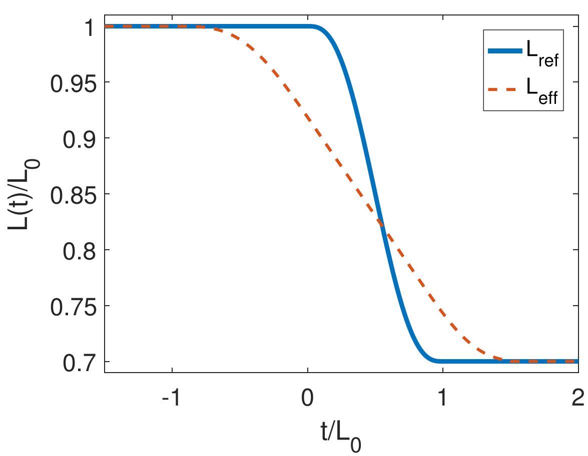

FIG. 1. A reference trajectory (blue solid line) given by Eq. (15) with $\epsilon = 0.3$ and $\tau/L_0 = 1$. The corresponding effective trajectory (orange dashed line) calculated from Eq. (13) gives the shortcut to adiabaticity.

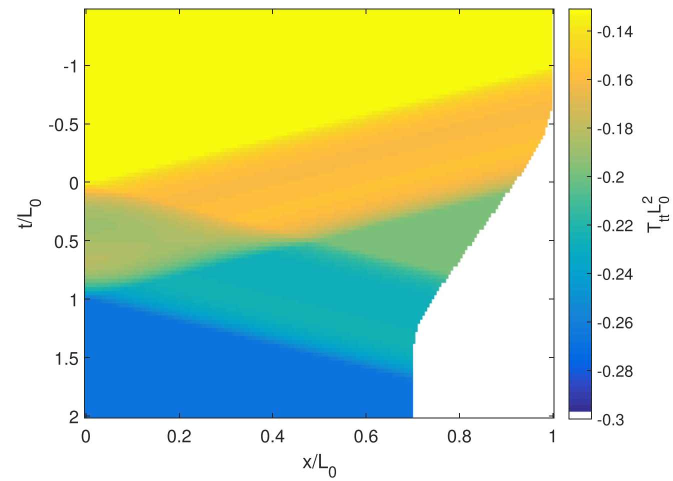

FIG. 2. Energy density for an adiabatic shortcut corresponding to the polynomial trajectory with length $L_1/L_0 = 0.7$ and $\tau/L_0 = 1$ from $t = -L_0$ to $t = L_1 + \tau$ and the field initially in the vacuum state. The energy density is a negative constant before and after the compression and it is smaller at the end.

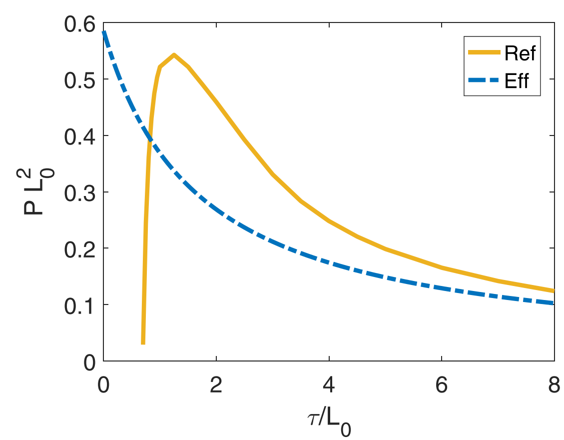

FIG. 4. Power for an Otto cycle as a function of the timescale, τ, implementing the reference (solid line) or effective STA trajectory (dashed line) for the expansion and compression strokes. The parameter used for the trajectory was $\epsilon = 0.3$, while the thermal baths used for the cycle had temperatures $T_0 L_0 = 1$ and $T_1 L_0 = 5$.